Influence of intensive parameters and assemblies on friction evolution during piston-cylinder experiments

Pierre Condamine, Simon Tournier, Bernard Charlier, Etienne Médard, Antoine Triantafyllou, Célia Dalou, Laurent Tissandier, Delphine Lequin, Camille Cartier, Evelyn Füri, et al.

Influence of intensive parameters and assemblies on friction evolution during piston-cylinder experiments

Authors

Pierre Condamine*[1], Simon Tournier[1], Bernard Charlier[2], Etienne Médard[3], Antoine Triantafyllou[5], Célia Dalou[1], Laurent Tissandier[1], Delphine Lequin[1], Camille Cartier[1], Evelyn Füri[1], Pete G. Burnard[1], Sylvie Demouchy[4], Yves Marrocchi[1]

Affiliations

[1]*Université de Lorraine, CNRS, CRPG, F-54000 Nancy, France*

[2]*Department of Geology, University of Liège, 4000 Sart Tilman, Belgium*

[3]*Université Clermont Auvergne, CNRS, IRD, OPGC, Laboratoire Magmas et Volcans, F-63000 Clermont-Ferrand, France*

[4]*Géosciences Montpellier, CNRS, Université de Montpellier, F-34095 Montpellier, France*

[5]*Geology laboratory of Lyon - Earth, Planets and Environment (LGL-TPE), Université Lyon 1, ENS de Lyon, CNRS, UMR 5276, Villeurbanne, France*

Correspondence (*)

pierre.condamine@univ-lorraine.fr

Abstract

Piston-cylinder assemblies exhibit inhomogeneous pressure distributions and biases compared to the theoretical pressure applied to the hydraulic press because of the thermal and mechanical properties of the assembly components. Whereas these effects can partially be corrected by conventional calibration, systematic quantification of friction values remain very sparse and results vary greatly among previous studies. We performed an experimental study to investigate the behavior

of the most common cell assemblies, i.e., talc ($Mg_3Si_4O_{10}(OH)_2$), NaCl, and $BaCO_3$, during piston-cylinder experiments to estimate the effects of pressure, temperature, run duration, assembly size, and assembly materials on friction values. Our study demonstrates that friction decreases with time and also partially depends on temperature but does not depend on pressure. We determined that friction decreases from 24 to 17% as temperature increases from 900 to 1300 °C when using talc cells, indicating a friction decrease of ~2% per 100 °C increase for 24-h experiments. In contrast, friction becomes independent of time above 1300 °C. Moreover, at a fixed temperature of 900 °C, friction decreases from 29% in 6-h runs to 21% in 48-h runs, corresponding to a decrease of friction of 0.2% per hour. Similar results obtained with NaCl cell assemblies suggest that friction is constant within error, from 8% in 9-h runs to 5% in 24-h runs. At 900 °C, possible steady-state friction values are only reached after at least 48 h, indicating that friction should be considered a variable for shorter experiments. We establish that assembly materials (and their associated thermomechanical properties) influence the friction correction more than the dimensions of the assembly parts. Finally, we show that the use of polytetrafluoroethylene film instead of conventional Pb foil does not modify friction, but significantly reduces the force required for sample extraction, thus increasing the lifetime of the carbide core, which in turn enhances experimental reproducibility.

Keywords

Experimental petrology | Piston-cylinder | Friction | Assembly | Calibration

1. Introduction

The piston-cylinder apparatus (Boyd and England 1960) is well established in experimental petrology and mineralogy for the synthesis of high-pressure and high-temperature geomaterials. Typical setups can attain pressures of 0.5–4 GPa and temperatures of 600–2000 °C, and special setups extend these ranges down to 0.3 GPa (e.g., Mirwald et al. 1975; Moore et al. 2008) and up to 2500 °C (Cottrell and Walker 2006). Piston-cylinders are thus particularly well suited to investigate material properties at crustal to upper mantle conditions on Earth and even at core conditions on smaller

planetary bodies. Furthermore, many thermodynamic models concerning the properties of the mantle and their evolution through geological time rely on experimental databases. It is thus critical to provide accurate experimental data with minimal uncertainties.

During high-pressure and high-temperature (*HP-HT*) piston-cylinder experiments, multiple factors can lead to important biases on the pressure applied to the sample. Laboratories worldwide employ various pressurization and heating procedures to reach the *P-T* conditions of interest, such as the commonly used hot piston-in and piston-out techniques, leading to noticeably different applied pressures (Johannes et al. 1971; Shimizu and Kushiro 1984; McDade et al. 2002). It has also been suggested that a fraction of the hydraulic pressure is not transmitted to the sample due to heterogeneous pressure distributions and/or frictional strain between the carbide core and the cell assembly (Tamayama and Eyring 1967; Edmond and Paterson 1971). These pressure losses can be characterized by the friction value *F* (in %), defined as the difference between the applied hydraulic pressure P_{app} and the effective pressure on the sample P_{eff}:

$$F = \left(\frac{P_{app}}{P_{eff}} - 1\right) \times 100 \quad (1)$$

The materials used in piston-cylinder cell assemblies vary widely depending on the purpose of the experiments (see Dunn 1993 for a review). For instance, different spacer and sleeve materials can be used around the sample, each possessing unique thermal and mechanical properties (Bell et al. 1971; Longhi 2005). Alumina is sometimes substituted for MgO spacers to complete graphite furnaces (Johannes et al. 1971; McDade et al. 2002); however, the different rheological properties of alumina and MgO (elasticity, ductility, hardness) can lead to over- and under-pressured zones around the sample. Furthermore, assemblies made with high-strength materials require greater pressure corrections than those made with low-strength materials (Johannes, 1978). It is therefore important to understand and quantify the role of material properties such as hardness, density, isothermal compressibility, and thermal expansion during *HP-HT* experiments.

Several studies have sought to (i) understand and model thermal uncertainties and reproducibility during piston-cylinder experiments (e.g., Watson et al. 2002; Médard et al. 2008) and (ii) estimate the friction correction required depending on cell materials, including the commonly used

talc, NaCl, and $BaCO_3$ pressure media (e.g., Fram and Longhi 1992; Bose and Ganguly 1995; McDade et al. 2002; Longhi 2005). However, the reproducibility of pressure and associated corrections (i.e., friction) during *HP-HT* experiments and which parameters control their evolution remain unclear. For example, Fram and Longhi (1992) claimed that the friction correction is highly dependent on pressure for $BaCO_3$ cells, whereas McDade et al. (2002) reported that friction is independent of temperature and pressure at 1000–1600 °C and 1.5–3 GPa. Therefore, the main objective of this study is to experimentally quantify the friction induced by the use of talc, NaCl, and $BaCO_3$ cells during piston-cylinder experiments. Whereas the use of talc cells is known to produce important pressure losses on the sample compared to the applied hydraulic pressure, friction values are only sparsely reported and vary widely (Johannes et al. 1971; McDade et al. 2002). Our second aim, then, is to understand and quantify the roles of experimental parameters (pressure, temperature, and experimental duration) and assembly materials and size on friction and its evolution during short- and long-duration experiments.

2. Methods

2.1. Experimental strategy

Experiments were performed on three different reactions. First, we chose the quartz-coesite transition for its shallow *P-T* slope (Bose and Ganguly 1995, and references therein), which limits biases due to thermal gradients. This simple reaction precludes problems observed in other commonly used transitions, such as synthesis of the starting material in the fayalite + quartz = ferrosilite transition (see Bohlen et al. 1980). In addition, the kinetics of this transition are remarkably fast (Lathe et al. 2005), allowing experiments to be performed over both short (2.5 h) and long durations (48 h), in turn allowing us to investigate the evolution of friction over time. We calibrated the quartz-coesite transition over a wide range of typical piston-cylinder temperatures, i.e., at 900 and 1300 °C, to understand the role of temperature on frictional issues in the three cell types (Figure 1). Second, we investigated the albite ($NaAlSi_3O_8$) = jadeite ($NaAlSi_2O_6$) + quartz (SiO_2) reaction at 800 and 1000 °C using $BaCO_3$ cells (Holland 1980). Third, we investigated the anorthite ($CaAl_2Si_2O_8$) + gehlenite ($Ca_2Al_2SiO_7$) + corundum (Al_2O_3) = kushiroite ($3CaAl_2SiO_6$) reaction (Hays 1966a, b) at a constant

pressure of ~1.3 GPa using talc cells to understand the role of pressure and assembly size (1/2" vs. 3/4") on friction at 1300 °C.

Because low-temperature and short-duration experiments exacerbate friction (Bose and Ganguly 1995), we performed additional experiments on the roles of assembly size and component materials at 900 °C during 6 h. These experiments included replacing the MgO sleeve around the capsule with an alumina sleeve, using a polytetrafluoroethylene (PTFE) film wrapping the cell, and using higher density MgO spacers (2.8 vs. 2.0 g/cm^3) in the graphite furnace (Table 1). A last series of experiments was performed on a new batch of assemblies (thicker talc cell, thinner Pyrex glass) at more conventional piston-cylinder conditions (1300 °C, 24 h) to understand the potential role of assembly part sizes on the generated friction (batch #2; Table 1, Figure 1d).

2.2. Starting materials

For the quartz-coesite calibration experiments, we used analytical grade amorphous SiO_2 (99.9 wt% purity) and added 6 wt% H_2O to each capsule with a micro syringe to enhance the reaction kinetics (Lathe et al. 2005). To study the kushiroite = anorthite + gehlenite + corundum reaction, we prepared a mixture based on the stoichiometry of the kushiroite, using analytical grade SiO_2, Al_2O_3, and $CaCO_3$ powders, ground in ethanol for 1 h, and then decarbonated in a furnace at 1200 °C during 24 h. The procedure was repeated to ensure complete decarbonation. Oxide powders were stored in an oven at 110 °C prior to capsule assembly. For the albite = jadeite + quartz reaction, the starting material consisted of a mixture of pure powdered crystals, validated by X-ray diffraction measurements on a Bruker D8-Advance diffractometer with CuKα radiations (ULiege). Proportions were set during mixture preparation, with 70 wt.% quartz, 20 wt.% jadeite and 10 wt.% albite. The powder's mixture was stored in an oven at 120°C prior to capsule assembly.

2.3. Experimental techniques

We performed 38 experiments on identical Voggenreiter Mavo LPC 250-300/50 end-loaded 12.7-mm (1/2") and 19.0-mm (3/4") piston-cylinders at three different institutes: the Centre de

Recherches Pétrographiques et Géochimiques (CRPG, Nancy, France) for talc cell assemblies, the Laboratoire Magmas et Volcans (LMV, Clermont-Ferrand, France) for NaCl cell assemblies, and the University of Liège (ULiège; Belgium) for $BaCO_3$ cell assemblies. The talc-based piston-cylinder assembly (Ceramic Substrates and Components Ltd.) comprised a talc cell wrapped in an outer PTFE film, a Pyrex cylinder, a graphite furnace, and inner MgO spacers (Figure 1a). The current was conducted to the graphite heater through a stainless-steel plug, which was electrically isolated with a pyrophyllite sleeve. The use of PTFE film instead of conventional Pb foil for the outer sleeve allows covering the base plug, which tends to drastically decrease the force required to extract the assembly at the end of an experiment from ~35 to ~5 kN, which in turn better preserves the carbide core from fracturing. PTFE is also a more environment- and health-friendly alternative compared to Pb and/or Mo-based lubricants. The NaCl cell assembly was similar to the talc cell assembly (Figure 1b). At ULiège, the assembly is composed of a $BaCO_3$ cell wrapped in Pb foil, a graphite furnace, and MgO spacers (Figure 1c). Additional details on assembly materials and dimensions are provided in Supplementary Materials 1. Calibrated $W_{74}Re_{26}$-$W_{95}Re_5$ thermocouples protected by a 4-bore alumina sleeve were used to control temperature to within 1 °C of the setpoint. Temperature gradients throughout the capsule are estimated to be about 20 °C (Sorbadere et al. 2013). The hot spot is located in the center of the capsule, implying a thermal gradient of about 10 °C/mm. To preclude perforation of the capsule, an Al_2O_3/MgO cap 0.6 mm thick was inserted between the capsule and the thermocouple. During experiments, the pressure was first increased to about 0.7 GPa (1/2" assemblies) or 0.3 GPa (3/4" assemblies) at room temperature. In all experiments, the temperature was then increased to 650 °C at 50 °C/min, held for 15 min to reach the target pressure, and then heated to the target temperature.

Several series of experiments were conducted to understand the role of assembly parts on friction in talc cells (Table 1). In experiments V32 and V42, we replaced the MgO sleeve with an alumina sleeve, a method used to preserve the experimental charge because alumina sleeves are harder and denser than MgO sleeves. We also investigated the role of the density of MgO spacers by replacing the conventional spacers (2.0 g/cm^3) with higher density spacers (2.8 g/cm^3) in experiments V109 and V117. In experiments V110 and V116, we tested a last batch of assemblies (batch #2) with

thicker talc cells (1.35 mm instead of 0.75 mm) and thinner Pyrex glass cylinders (1 mm instead of 1.6 mm; see details in Supplementary Materials 1). Finally, in experiments V39 and V107, Pb foil was used instead of the PTFE film.

For quartz-coesite transition experiments, $Au_{80}Pd_{20}$ capsules (4 mm high) were used to limit water loss (Gaetani and Grove 1998; Kägi et al. 2005). For the kushiroite reaction, Pt capsules (4 mm high) were employed. For the albite = jadeite + quartz reaction, graphite containers (3.75 mm high) were used. At the end of each experiment, the capsule was cut in half longitudinally using a wire saw, mounted in epoxy, and polished to 0.25 µm on nylon pads with diamond pastes.

2.4. Analytical techniques

Experimental run products of the kushiroite reaction were analyzed with a JEOL JSM-6510 scanning electron microscope (SEM) at CRPG using an accelerating voltage of 15 kV, a beam current of 10 nA, and a spot size of ~ 1 µm. Back-scattered electron images of experimental run products of the albite = jadeite + quartz reaction were acquired on the QEMSCAN FEI Quanta 650F at RWTH Aachen (Germany).

Raman spectroscopy was used to determine the nature of silica polymorphs in all experiments. Raman spectra were acquired using a LabRAM HR spectrometer (Horiba Jobin Yvon) at GeoRessources (Nancy, France). The spectrometer is equipped with a 600 gr/mm grating and an edge filter. The confocal hole aperture is 500 µm and the slit aperture is 100 µm. The excitation beam (wavelength, 514.53 nm; power, 200 mW) was produced by a Stabilite 2017 Ar+ laser (Spectra Physics, Newport Corporation) and focused on the sample using a 50× objective. The acquisition time (2 s) and the number of accumulated spectra (20) were chosen to optimize the signal-to-noise ratio. All spectra were recorded over Raman shifts of 150–1400 cm^{-1}. Quartz and coesite were identified by their respective peaks at 470 and 520 cm^{-1}.

3. Experimental textures and products

Experimental conditions and results of quartz-coesite, kushiroite, and albite reactions are reported in Table 1, and calculated frictions are reported in Table 2. Pictures of typical run products are provided in Supplementary Material 2. In quartz-coesite experiments, coesite was always observed with variable amounts of quartz. Coesite mainly occurs as straight veins in the euhedral quartz matrix, with no preferential orientation. In kushiroite reaction experiments, grain growth was observed in all runs, with anhedral grains ranging from 20 to 50 μm. Kushiroite mainly appears near corundum and anorthite, replacing gehlenite. In runs in which kushiroite was observed (V106 and V113), anorthite, gehlenite and corundum were still present after 24 h.

Non-negligible amounts of the low-pressure phases in the three investigated reactions (i.e., quartz, anorthite + gehlenite + corundum, and albite) persisted after the transition reaction occurred. This result is consistent with Hays (1966a, b), who observed low-pressure phases persisting above the transition to kushiroite, indicating a continuous reaction over a pressure interval of a few kilobars. In contrast to our experiments with a transitional pressure interval of ~0.1 GPa, Bose and Ganguly (1995) found only either quartz or coesite in their experiments with a pressure interval of ~0.05 GPa. We could not estimate modal abundances from our experimental textures due to significant sample losses during cold decompression.

4. Roles of intensive parameters on friction

In the following sections, experiments from Bose and Ganguly (1995) were chosen as the reference pressure (P_{eff}) for the quartz-coesite system. They indeed showed that after 30 h, the friction is null in their assemblies, based on crossed calibrations using high pressure vessel experiments. In the quartz-coesite system, our experiments at both 900 and 1300 °C allow us to investigate the role of temperature on friction (Figure 2). In 24-h experiments in talc cells, the quartz-coesite transition occurred between applied pressures of 3.68 and 3.77 GPa at 900 °C and between 3.77 and 3.87 GPa at 1300 °C. In contrast, Bose and Ganguly (1995) observed the transition at 3.00 and 3.28 GPa at 900 and 1300 °C, respectively, in CsCl cells. Taking their values as the effective pressure on the sample,

our results indicate friction values (F) for talc cells of 24.1% at 900 °C and 16.5% at 1300 °C (Table 1). A linear fit to these values (Figure 2) shows that friction decreases by about 2% when temperature increases by 100 °C in 24-h experiments. In NaCl cells, the quartz-coesite transition occurred between 3.11 and 3.21 GPa at 900 °C (F = 5.4 ± 3.0%) and between 3.41 and 3.46 GPa at 1300 °C (F = 4.8 ± 3.0%), indicating no friction evolution within error. In $BaCO_3$ cells, the albite = jadeite + quartz reaction occurred between 2.35 and 2.4 GPa at 800 °C and between 2.8 and 2.9 GPa at 1000 °C. Compared to 2.16 and 2.69 GPa at 800 and 1000 °C obtained in Holland (1980), F = 10.2 ± 4.3 and 6.1 ± 3.4%, respectively, indicating no friction evolution in this range of temperature.

Our experiments on the kushiroite = anorthite + gehlenite + corundum reaction were conducted at 1300 °C to understand the role of pressure on the friction value in talc cells. In 1/2" assemblies, this transition occurred between applied pressures of 1.45 and 1.54 GPa in 24-h experiments. According to the equation of Hays (1966a), the reference pressure for this transition is 1.3 GPa, resulting in a friction value of 15.1 ± 4.3%.

This value is identical, within errors, to the friction value obtained from the quartz-coesite transition at the same temperature (16.6 ± 3.2%), implying that the friction value is independent of confining pressure at identical temperatures and experimental durations. This result is partially consistent with McDade et al. (2002), who argued that the friction correction is independent of pressure and temperature at 1000–1600 °C and 1.5–3.2 GPa in $BaCO_3$ cells. However, our results show that friction is temperature dependent in talc cells, decreasing by 2% over a temperature increase of 100 °C between 900 and 1300 °C. This difference can be explained by the slower stress accommodation of talc compared to NaCl and $BaCO_3$ cells due to its higher strength. It is also possible that friction becomes more strongly temperature dependent at low temperature (<1000 °C). We speculate that stress accommodation is fast enough above 1000 °C to be undetectable under these experimental conditions.

5. Friction evolution

We performed experiments on the quartz-coesite reaction at 900 °C and over various run durations between 2.7 and 48 h to investigate the evolution of friction during a single run (Figure 3).

In talc cells, the transition occurred at progressively lower applied pressures with increasing run duration (Table 1); friction thus evolved from 33.8 ± 3.4% after 2.7 h to 30.7 ± 3.3% after 4.5 h, 27.3 ± 3.3% after 6 h, 24.1 ± 3.2% after 24 h, and to 20.9 ± 3.2% after 48 h (Figure 3). Whereas a linear fit to the data for longer durations (≥6 h) indicates that friction decreases by ~2% every 10 h, a power-law fit better describes the full dataset. This may explain the ubiquitous presence of quartz in all experiments conducted in talc cells via the early crystallization of quartz from the amorphous SiO_2 starting material at low effective pressures and its subsequent metastability. In contrast, in talc cell assemblies at 1300 °C, friction did not evolve between 6- and 24-h duration experiments, indicating that a frictional steady state was achieved within less than 6 h.

In NaCl cells at 900 °C, the apparent pressure of the quartz-coesite transition decreased from between 3.21 and 3.30 GPa after 9 h (F = 8.4 ± 3.1%) to between 3.11 and 3.21 GPa after 24 h (F = 5.4 ± 3.0%), indicating no friction evolution within error, contrary to what is reported in talc cells over longer duration experiments. The friction decrease in talc cell is however consistent with the data of Bose and Ganguly (1995) in CsCl cell assemblies (both 1/2" and 3/4"), which show that friction decreased from 6.6% after 2 h to negligible after 35 h, or by ~2% every 10 h (Figure 3).

6. Thermomechanical properties of assembly components

Alumina sleeve

Experiments V32 and V42 (Table 1) were performed at 900 °C and applied pressures of 3.87 and 3.97 GPa, respectively, with an alumina sleeve around the capsule instead of a conventional MgO sleeve. In both experiments, only quartz was observed, and the pressure limitation of the carbide core precludes experiments at pressures above ~4 GPa. Thus, the minimum friction observed using alumina sleeves is >32.3% (Figure 4). However, the main advantage of alumina sleeves is that the sample capsule conserves its cylindrical shape, preventing excessive deformation during quenching and cold depressurization, a net advantage when working with single crystals. McDade et al. (2002) obtained a friction value of 3.6% in NaCl cells by using an alumina sleeve and Alsimag (Al_2O_3) plugs to fill the tapered graphite furnace. Given the high density and hardness of Alsimag, these plugs are better

pressure transmitters than the crushable MgO used in our assembly setup. The combination of an alumina sleeve with MgO spacers thus greatly decreases pressure transmission and should only be used to limit fracturing of the experimental product in cases requiring particular care for the capsule.

Density of MgO spacers

Experiments V109 and V117 made with talc-Pyrex assemblages were conducted 900 °C and applied pressures of 3.68 and 3.77 GPa, respectively, with higher density MgO spacers (2.8 vs. the usual 2.0 g/cm^3). Both coesite and quartz were observed in V117, positioning the apparent quartz-coesite transition at 3.72 GPa. The friction obtained using these MgO spacers (24.1 ± 3.2%; Figure 4) is identical within error to that obtained using the standard assembly under the same conditions (27.3 ± 3.3%). This result demonstrates that the densities of assembly components does not significantly affect the effective sample pressure. This however further highlights that the Alsimag spacers used by McDade et al. (2002) are a good pressure medium, as they achieved a friction value of only 3.6%.

Assembly size (1/2” vs. 3/4”)

Kushiroite reaction experiments were performed in both 1/2” and 3/4” assemblies at 1300 °C for 24 h (Table 1). The calculated friction values are identical within errors, i.e., 15.1 ± 4.3% and 15.9 ± 4.4% for the 1/2” and 3/4” assemblies, respectively (Figure 3), suggesting that the size of assembly parts has a negligible effect on friction compared to assembly materials (and their associated thermomechanical properties).

Experiments V110 and V116 were performed using assemblies with thicker talc cells and thinner Pyrex sleeves (‘batch #2’, see Supplementary Materials 1 for size details). The friction determined for this assembly (16.6 ± 3.2%) is identical to that for the standard assembly (16.6 ± 3.2%) at 1300 °C for 24 h (Figure 4), further demonstrating that assembly materials have a stronger influence on friction than their sizes.

Pb foil vs PTFE foil

Experiments V107 and V39 were performed at 900 °C and applied pressures of 3.77 and 3.87 GPa, respectively, using talc cells and standard Pb foil instead of the PTFE film used elsewhere in this study (excluding ULiège experiments, Table 1). Coesite was only observed in experiment V39, implying that friction (27.3 ± 3.3%) was identical within errors to that using a PTFE-wrapped assembly (27.3 ± 3.3%; Figure 4). As previously mentioned, the key advantage of using PTFE film instead of Pb foil is the preservation of the carbide core of the pressure plates. The steel base plug, surrounded by pyrophyllite, is frequently stuck in the carbide core when removing the assembly, especially after experiments run at pressures above 2.0 GPa. The use of Pb foil precludes covering the base plug to avoid melting the Pb at the contact point with the thermocouple plate, which can electrically short-circuit the experiment. Therefore, the use of PTFE film is recommended to limit the development of fractures within the carbide core, which will both extend the life of the carbide core and enhance pressure reproducibility over that lifetime.

7. Implications for pressure reproducibility during piston-cylinder experiments

In this section, we provide general recommendations to improve pressure and temperature reproducibility during piston-cylinder experiments. These recommendations can be adapted, depending on the capsule material and the scientific purpose, e.g., for oxygen-fugacity buffering or volatile-bearing experiments. These recommendations are depicted in *P-T-t* space in the form of preferential practices in Figure 5.

At temperatures above 1600 °C, the NaCl cell is no longer usable because of the melting point of NaCl. Consequently, only talc or $BaCO_3$ cells should be used for very-high temperature experiments. Talc cells require a very-high frictional correction factor, regardless of *P-T-t* conditions (Table 2) and should thus be avoided in very high pressure experiments (>3 GPa) because the carbide core could suffer from excessive applied pressure. To generate pressures above 3 GPa, we thus recommend using NaCl cells below 1600 °C because they exhibit the lowest friction corrections (Figures 2 and 3) or $BaCO_3$ cells at higher temperatures. For experimental durations of a few to ~48 h

and pressures below 3 GPa, talc cells are as competent as NaCl and $BaCO_3$ cells because they all show similar frictional evolution with time. However, for short experiments (≤6 h), we recommend using NaCl or $BaCO_3$ cells as the decrease in friction value with time is comparable and because the friction in talc cells is much greater (following a power law) in shorter duration experiments (Figure 3). As described in section 5, this could lead to unexpectedly low effective pressures, promoting the crystallization and metastability of low-pressure phases. For experiments longer than 48 h (and below 1600 °C), we recommend using NaCl cells: whereas friction becomes negligible in CsCl cells after ~30 h (Bose and Ganguly 1995), the behavior of talc cells in experiments longer than 48 h remains unclear. Therefore, for temperatures above 1600 °C and durations longer than 48 h, we recommend using $BaCO_3$ cells because of their lower frictional correction compared to talc cells.

8. Conclusions

We determined the effects of pressure, temperature, time and assembly parts (materials and size) on the frictional correction factors to be applied to piston-cylinder experiments using talc cell assemblies. Whereas pressure calibrations in most laboratories assume a single value for friction correction for a given assembly, our study demonstrate that friction is time- and temperature-dependent, and particularly elevated friction can be produced for short experiments at low temperature, especially for talc-cell assemblies. Whereas the size of assembly parts has a negligible effect on friction, different sleeve and spacer materials (here, MgO vs. alumina) can significantly change the friction factors. Friction decreases by about 2% per 100 °C increase between 900 and 1300 °C at a given duration. Experimental duration also has a strong effect on the friction value at low temperatures, with friction decreasing by about 0.2% per hour at 900 °C; this effect is not observed at 1300 °C. In contrast to CsCl cells, in which friction becomes negligible after around 30–35 h, the friction in talc cells, although decreasing with increasing run duration, is never negligible, especially at low temperatures. Therefore, special care must be taken for low-temperature experiments (roughly <1000 °C) using talc cells, especially at short durations, because the slow stress accommodation of the assembly results in slow frictional evolution during the first several hours. Other key parameters not studied here may also critically affect friction and its evolution. In particular, the quality of the carbide

core and the development of fractures are expected to influence the friction generated on the assembly. A more systematic calibration procedure including the status of the core is thus necessary to provide a complete model of friction and its evolution during an experiment. This is fundamental for phase relationship experiments or the quest for low-degree melts from mantle lithologies, for which accurate and reproducible *P-T* conditions are essential. Furthermore, a dynamic model for friction correction should be developed to ensure pressure reproducibility among *HP-HT* petrological studies.

Acknowledgments

The authors thank M.-C. Caumon for technical assistance with Raman analyses and P. Baillot for his technical expertise in the laboratory. We also thank K. Koga and F. Faure for fruitful discussions. P.C. thanks C. McCammon for fundamental advice when building the piston-cylinder laboratory at CRPG. This study was mainly financed by l'Agence Nationale de la Recherche through grant ANR INDIGO (ANR-14-CE33-0011). C. Dalou and E. Füri were supported by the European Research Council (ERC) under the European Union's Horizon 2020 research and innovation program (grant agreement no. 715028). B. Charlier is a Research Associate of the Belgian Fund for Scientific Research-FNRS. A. Triantafyllou was supported by the FRS-FNRS for the PROBARC project (Grant CR n°1. B. 414.20F). This is CRPG contribution no. 2747.

References

Bell, P., Mao, H., and England, J. (1971) A discussion of pressure distribution in modern solid-pressure-media apparatus. Carnegie Institution of Washington, Yearbook, 70, 277–281.

Bohlen, S.R., Essene, E.J., and Boettcher, A.L. (1980) Reinvestigation and application of olivine-quartz-orthopyroxene barometry. Earth and Planetary Science Letters, 47, 1–10.

Bose, K., and Ganguly, J. (1995) Quartz-coesite transition revisited; reversed experimental determination at 500-1200 degrees C and retrieved thermochemical properties. American Mineralogist, 80, 231–238.

Boyd, F.R., and England, J.L. (1960) Apparatus for Phase-Equilibrium Measurements at Pressures up to 50 Kilobars and Temperatures up to 1750°C. Journal of Geophysical Research, 65, 741–748.

Cottrell, E., and Walker, D. (2006) Constraints on core formation from Pt partitioning in mafic silicate liquids at high temperatures. Geochimica et Cosmochimica Acta, 70, 1565–1580.

Dunn, T. (1993) The Piston-Cylinder Apparatus. In R.W. Luth, Ed., Experiments at High Pressure and Applications to the Earth's Mantle Vol. 21, pp. 39–94.

Edmond, J.M., and Paterson, M.S. (1971). Strength of solid pressure media and implications for high pressure apparatus. Contributions to Mineralogy and Petrology 30, 141–160.

Fram, M.S., and Longhi, J. (1992) Phase equilibria of dikes associated with Proterozoic anorthosite complexes. American Mineralogist, 77, 605–616.

Gaetani, G.A., and Grove, T.L. (1998) The influence of water on melting of mantle peridotite. Contributions to Mineralogy and Petrology, 131, 323–346.

Hays, J.F. (1966a). Lime-Alumina-Silica. Year book - Carnegie Institution of Washington 65, 234–239.

Hays, J.F. (1966b) Stability and properties of the synthetic pyroxene CaAl2SiO6. American Mineralogist, 51, 1524–1529.

Holland, T.J.B. (1980) The reaction albite = jadeite+quartz determined experimentally in the range 600–1200 ° C. American Mineralogist, 65, 129–134.

Johannes, U. (1978) Pressure comparing experiments with NaCl, AgCl, talc, and pyrophyllite assemblies in a piston cylinder apparatus. Neues Jahrbuch für Mineralogie Monatshefte, 84–92.

Johannes, W., Bell, P.M., Mao, H.K., Boettche.Al, Chipman, D.W., Hays, J.F., Newton, R.C., and Seifert, F. (1971) Interlaboratory comparison of piston-cylinder pressure calibration using albite breakdown reaction. Contributions to Mineralogy and Petrology, 32, 24-.

Kägi, R., Müntener, O., Ulmer, P., and Ottolini, L. (2005) Piston-cylinder experiments on H2O undersaturated Fe-bearing systems: An experimental setup approaching fO2 conditions of natural calc-alkaline magmas. American Mineralogist, 90, 708–717.

Lathe, C., Koch-Müller, M., Wirth, R., Van Westrenen, W., Mueller, H.-J., Schilling, F., and Lauterjung, J. (2005) The influence of OH in coesite on the kinetics of the coesite-quartz phase transition. American Mineralogist, 90, 36–43.

Longhi, J. (2005) Temporal stability and pressure calibration of barium carbonate and talc/pyrex pressure media in a piston-cylinder apparatus. American Mineralogist, 90, 206–218.

McDade, P., Wood, B.J., Van Westrenen, W., Brooker, R., Gudmundsson, G., Soulard, H., Najorka, J., and Blundy, J. (2002) Pressure corrections for a selection of piston-cylinder cell assemblies. Mineralogical Magazine, 66, 1021–1028.

Médard, E., McCammon, C.A., Barr, J.A., and Grove, T.L. (2008) Oxygen fugacity, temperature reproducibility, and H2O contents of nominally anhydrous piston-cylinder experiments using graphite capsules. American Mineralogist, 93, 1838–1844.

Mirwald, P.W., Getting, I.C., and Kennedy, G.C. (1975) Low-friction cell for piston-cylinder high-pressure apparatus. Journal of Geophysical Research (1896-1977), 80, 1519–1525.

Moore, G., Roggensack, K., and Klonowski, S. (2008) A low-pressure–high-temperature technique for the piston-cylinder. American Mineralogist, 93, 48–52.

Shimizu, N., and Kushiro, I. (1984) Diffusivity of oxygen in jadeite and diopside melts at high pressures. Geochimica et Cosmochimica Acta, 48, 1295–1303.

Sorbadere, F., Médard, E., Laporte, D., and Schiano, P. (2013) Experimental melting of hydrous peridotite-pyroxenite mixed sources: Constraints on the genesis of silica-undersaturated magmas beneath volcanic arcs. Earth and Planetary Science Letters, 384, 42–56.

Tamayama, M., and Eyring, H. (1967). Study of Pressure Calibration and Pressure Distribution in a Piston-Cylinder High Pressure Press. Review of Scientific Instruments 38, 1009–1018.

Watson, E.B., Wark, D.A., Price, J.D., and Van Orman, J.A. (2002) Mapping the thermal structure of solid-media pressure assemblies. Contributions to Mineralogy and Petrology, 142, 640–652.

Figure captions

Figure 1. Schematic diagrams of the four different piston-cylinder cell assemblies used in this study. a) talc cell assembly used at CRPG (Nancy), b) NaCl cell assembly used at LMV (Clermont-Ferrand), c) $BaCO_3$ assembly used at ULG (Liège), d) batch #2 of the talc cell assembly used at CRPG, using a thicker cell and thinner Pyrex sleeve compared to *a*. The talc cell is 0.75 mm thick in *a* against 1.35 mm in *d*. Contrary to other assemblies, no Pyrex glass is present in the $BaCO_3$ cell assembly and a Pb film is used instead of PTFE to wrap the cell. See Supplementary Materials 1 for additional details.

Figure 2. Friction evolution as a function of temperature for 24 h experiments in 1/2" cell assemblies. The durations of experiments from McDade et al. (2002) were 22 h. Linear fits describe the change in friction as a function of temperature (°C): $F = -0.019T + 40.991$ for talc cells; $F = -0.006T + 10.370$ for NaCl cells; $F = -0.020T + 26.463$ for $BaCO_3$ cells.

Figure 3. Evolution of the friction value as a function of experimental duration. B&G1995 data correspond to the study of Bose and Ganguly (1995), performed at 900 °C with CsCl cells. At 900 °C, the friction value decreases of about 2 % every 10 h for experimental durations > 6 h. At 1300 °C, no friction decrease is observed between 6 and 24 h. Lower pressure (kushiroite experiments) and sizing of assemblies (1/2" and 3/4") do not seem to have a critical influence on the friction value and its evolution. The slope of the friction decrease observed in NaCl cell assemblies is comparable to the slope observed in Bose and Ganguly (1995).

Figure 4. Variations in friction with changes in assembly size and components, relative to experiments performed using the assembly shown in Figure 1a (talc cell, MgO sleeve, PTFE film, 2.0 g/cm^3 MgO spacers) at 900 °C for 6 h and 1300 °C for 24 h (1/2" assembly). 'Alumina sleeve' indicates that the regular MgO sleeve around the capsule was replaced by an alumina sleeve. 'Pb foil' indicates that the cell was wrapped in standard Pb foil instead of the PTFE film used throughout this study. 'MgO spacers' indicates that higher density MgO spacers (2.8 g/cm^3) were used within the

graphite furnace (including the sleeve around the capsule). 'Assembly batch #2' indicates the assembly shown in Figure 1d, using a thicker talc cell and thinner Pyrex sleeve than those in the regular assembly (Figure 1a). See Supplementary Materials 1 for details. Note that the friction reported for 'Alumina sleeve' is a minimum value because coesite was not observed in this series of experiments due to the pressure limitations of the press and carbide core.

Figure 5. Recommended cell types for piston-cylinder experiments as a function of pressure, temperature, and experimental duration. Note that the duration axis is not linear. These general recommendations limit the uncertainty on pressure and its evolution during *HP-HT* experiments, except for avoiding NaCl cells in experiments at very high temperature (>1600 °C) because the NaCl cell no longer acts as an electrical insulator. See discussion in section 7 for further details. Cell types are recommended as 'best > intermediate > worst' according to the color scale at bottom right.

Table 1

Experimental conditions and results

Assembly	T (°C)	Duration (h)	Run	P_{app} (GPa)	Product
Talc cell experiments (CRPG laboratory)					
PTFE - Talc - Pyrex - C - MgO	900	2.7	V130	3.97	qz
			V16	4.06	qz + co
		4	V10	3.87	qz
		5	V19	3.97	qz + co
		6	V108	3.77	qz
		15	V55	3.87	qz + co
			V41	3.77	qz
		24	V38	3.87	qz + co
			V30	3.68	qz
			V24	3.77	qz + co
		48	V33	3.58	qz
			V56	3.68	qz + co
	1300	6	V37	3.77	qz
		24	V18	3.87	qz + co
			V22	3.77	qz
			V57	3.87	qz + co
			V114	1.45	an + gh + crn
			V113	1.54	kush + an + gh + crn
PTFE - Talc - Pyrex - C - Al_2O_3	900	6	V32	3.87	qz
			V42	3.97	qz
Pb - Talc - Pyrex - C - MgO	900	6	V107	3.77	qz
			V39	3.87	qz + co
PTFE - Talc - Pyrex - C - MgO (2800 kg/m^3)	900	6	V109	3.68	qz
			V117	3.77	qz + co
PTFE - Talc - Pyrex - C - MgO (batch #2)	1300	24	V110	3.77	qz
			V116	3.87	co
PTFE - Talc - Pyrex - C - MgO (3/4")	1300	24	V112	1.46	an + gh + crn
			V106	1.55	kush + an + gh + crn
NaCl cell experiments (LMV laboratory)					
PTFE - NaCl - Pyrex - C - MgO	900	9	PC/2014/11	3.21	qz
		24	PC/2014/14	3.30	qz + co
			Cal-LMV-03	3.11	qz
			Cal-LMV-01	3.21	qz + co
	1300	24	Cal-LMV-02	3.41	qz
			Cal-LMV-04	3.46	qz + co
BaCO3 cell experiments (ULG laboratory)					
Pb - $BaCO_3$ - C - MgO	800	24	A070	2.35	ab
			A058	2.40	jd + qz
	1000	24	A073	2.80	ab
			A060	2.90	jd + qz

469 **Table 2**

Friction values

Size (")	T (°C)	Duration (h)	P_{app}	ΔP_{app}	P_{eff}	ΔP_{eff}	F (%)	ΔF	Comment
Talc cell (CRPG laboratory)									
Friction as a function of temperature									
	900		3.72	0.10	3.00	0.05	24.1	3.2	
	1000[a]		3.75	0.10	3.07	0.06	22.0	3.2	
1/2	1100[a]	24	3.77	0.10	3.14	0.06	20.1	3.2	
	1200[a]		3.79	0.10	3.21	0.06	18.3	3.2	
	1300		3.82	0.10	3.28	0.07	16.6	3.2	
Friction as a function of duration									
		2.7	4.01	0.10	3.00	0.05	33.8	3.4	
		4.5	3.92	0.10	3.00	0.05	30.7	3.3	
	900	6	3.82	0.10	3.00	0.05	27.3	3.3	
1/2		15	3.82	0.10	3.00	0.05	27.3	3.3	
		24	3.72	0.10	3.00	0.05	24.1	3.2	
		48	3.63	0.10	3.00	0.05	20.9	3.2	
	1300	6	3.82	0.10	3.28	0.07	16.6	3.2	
		24	3.82	0.10	3.28	0.07	16.6	3.2	
Friction as a function of pressure and assembly size									
1/2	1300	24	1.50	0.10	1.30	0.03	15.1	4.3	
3/4			1.51	0.06	1.30	0.03	15.9	4.4	
Friction as a function of assembly parts									
			3.82	0.10	3.00	0.05	27.3	3.3	Standard calibration (900 °C, 6 h)
	900	6	> 3.97		3.00	0.05	> 32.2		Alumina sleeve
			3.82	0.10	3.00	0.05	27.3	3.3	Pb foil
1/2			3.72	0.10	3.00	0.05	24.1	3.2	MgO spacers density
	1300	24	3.82	0.10	3.28	0.07	16.6	3.2	Standard calibration (1300, 24 h)
			3.82	0.10	3.28	0.07	16.6	3.2	Assembly batch #2
NaCl cell (LMV laboratory)									
1/2	900	9	3.25	0.10	3.00	0.05	8.4	3.1	
1/2		24	3.16	0.10	3.00	0.05	5.4	3.0	
1/2	1300	24	3.38	0.10	3.28	0.07	4.8	3.0	
$BaCO_3$ cell (ULG laboratory)									
1/2	800	24	2.38	0.10	2.16	0.05	10.2	4.3	
1/2	1000		2.85	0.10	2.69	0.05	6.1	3.4	

P_{app} and P_{eff} represent the pressure (GPa) applied by the press and the pressure on the sample, respectively. F represents the friction in %. ΔP_{app}, ΔP_{eff} and ΔF are 2σ standard deviations of applied pressure, sample pressure and friction, respectively.

[a]Values from the linear fit in Figure 2.

470

471

472 **Figure 1**

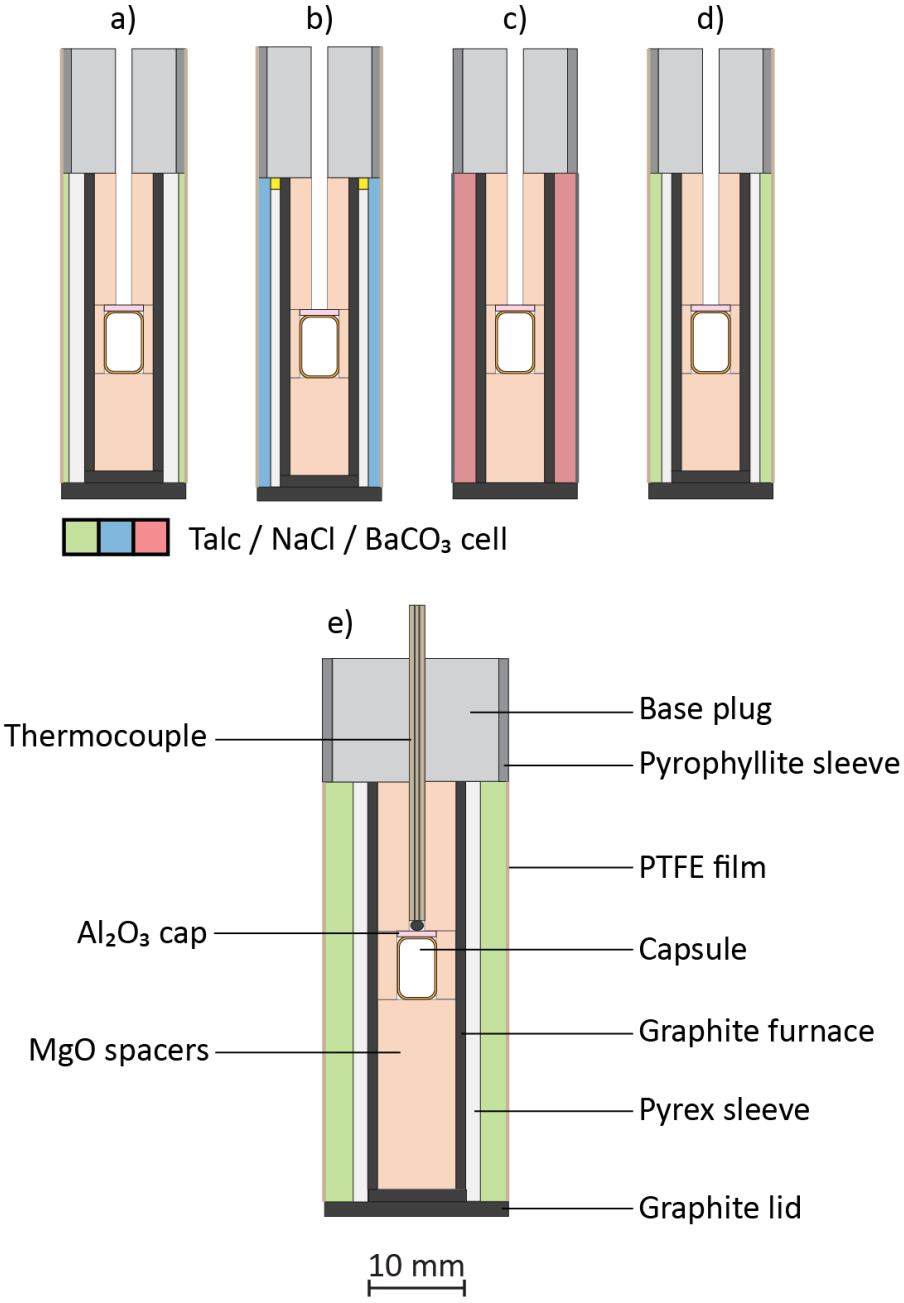

473

474

475 **Figure 2**

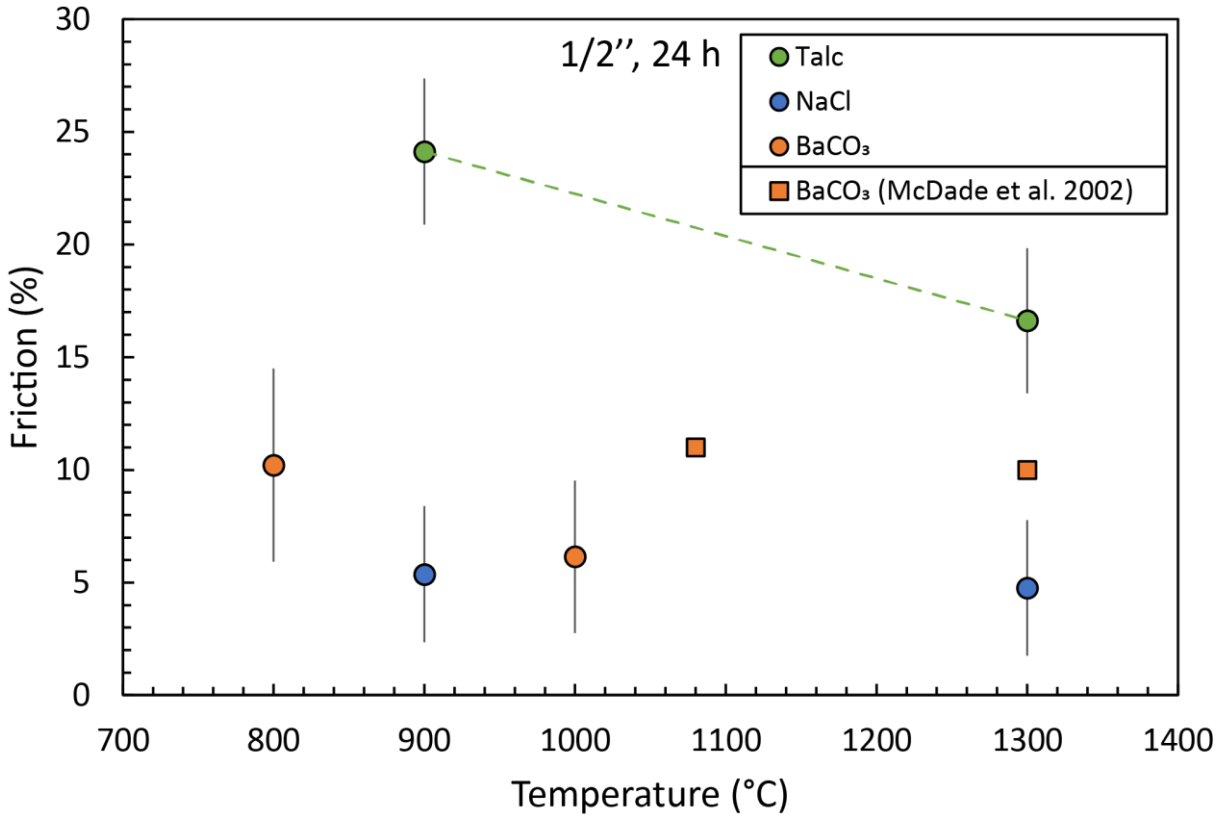

476

477

Figure 3

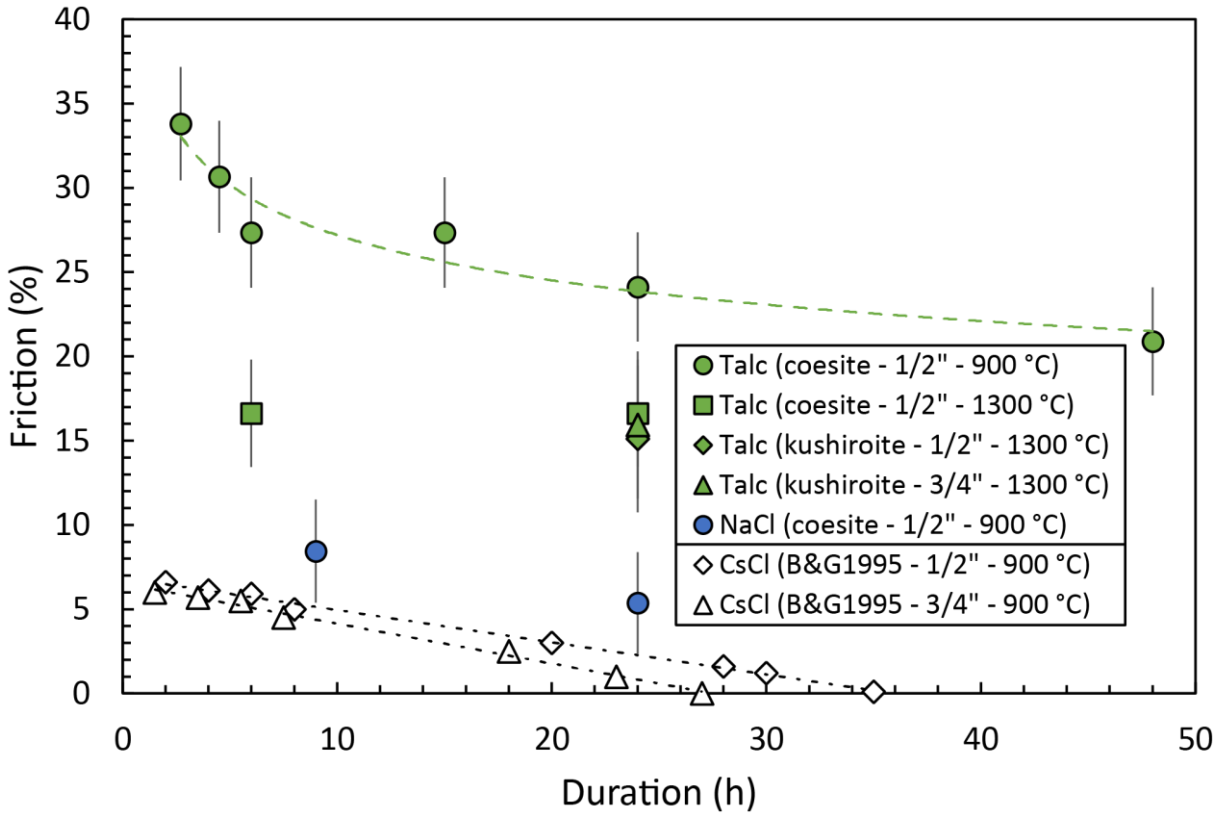
Friction (%)
Duration (h)
0
5
10
15
20
25
30
35
40
0
10
20
30
40
50
Talc (coesite - 1/2" - 900 °C)
Talc (coesite - 1/2" - 1300 °C)
Talc (kushiroite - 1/2" - 1300 °C)
Talc (kushiroite - 3/4" - 1300 °C)
NaCl (coesite - 1/2" - 900 °C)
CsCl (B&G1995 - 1/2" - 900 °C)
CsCl (B&G1995 - 3/4" - 900 °C)

Figure 4

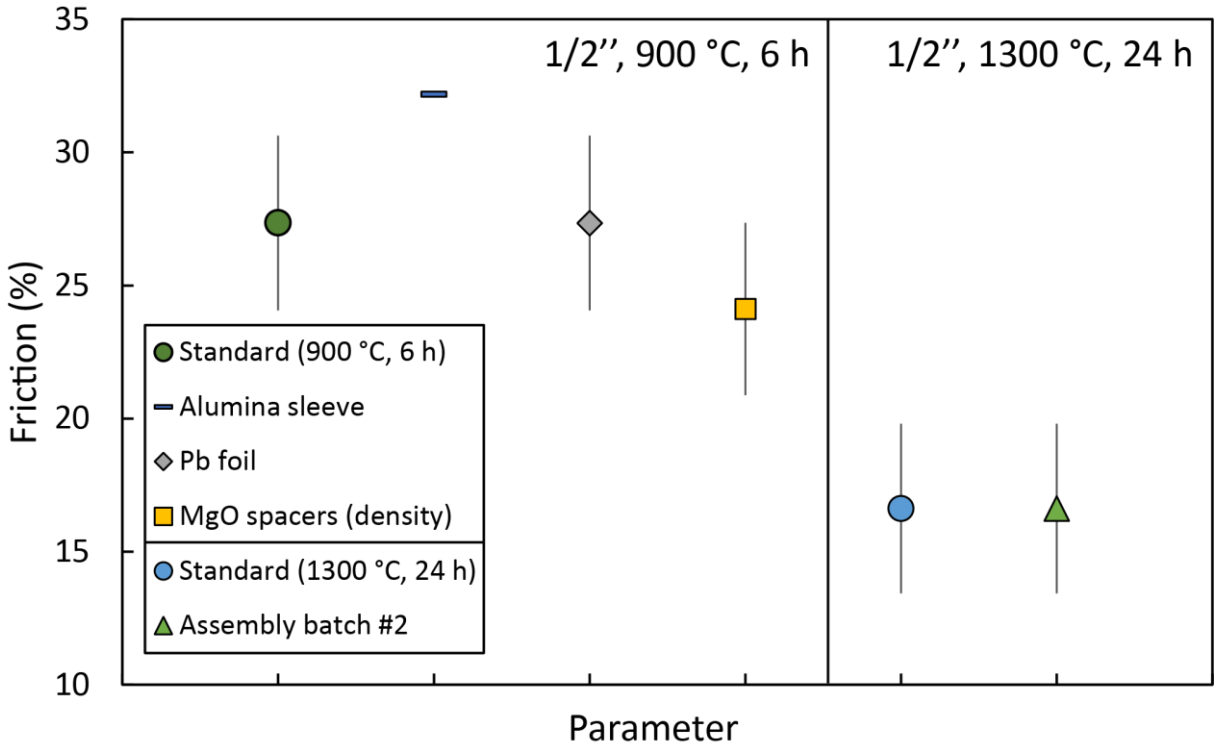
1/2'', 900 °C, 6 h
1/2'', 1300 °C, 24 h
Friction (%)
35
30
25
20
15
10
Standard (900 °C, 6 h)
Alumina sleeve
Pb foil
MgO spacers (density)
Standard (1300 °C, 24 h)
Assembly batch #2
Parameter

484 **Figure 5**

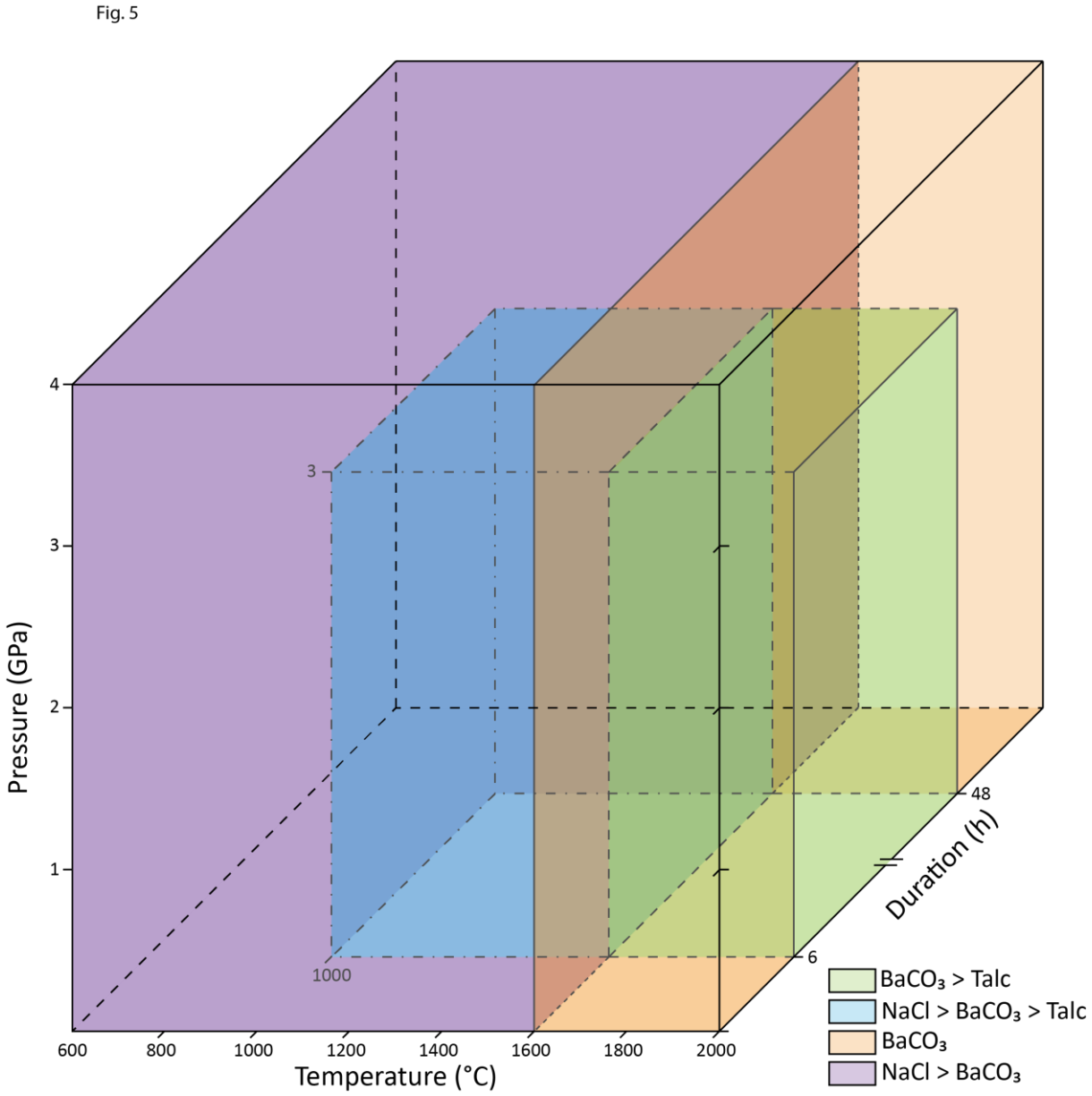

485

486

Supplementary Material

Influence of intensive parameters and assemblies on friction evolution during piston-cylinder experiments

P. Condamine, S. Tournier, B. Charlier, E. Médard, A. Triantafyllou, C. Dalou, L. Tissandier, D. Lequin, C. Cartier, E. Füri, P. Burnard, S. Demouchy, Y. Marrocchi

List of Supplementary Figures

Supplementary Material 1: Assembly sizes.

Supplementary Material 2: Pictures of typical run products from the three reactions investigated. a) Reflected light microscope image of the reaction quartz (Qz) - coesite (Co) in V18 (3.87 GPa, 1300 °C, 24 h). b) Back-scattered electron image of the reaction anorthite (An) + gehlenite (Gh) + corundum (Crn) = kushiroite (Ku) in V113 (1.54 GPa, 1300 °C, 24 h). c) Back-scattered electron image of the reaction jadeite (Jd) + quartz (Qz) = albite (Ab) in A070 (2.35 GPa, 800 °C, 24 h).

500 **Supplementary Material 1**

		CRPG (a)	CRPG (b)	LMV (c)	ULG (d)	CRPG (e)
Piston cylinder diameter	inch	1/2"	1/2"	1/2"	1/2"	3/4"
	mm	12.7	12.7	12.7	12.7	19.1
Pressure vessel height		52.00	52.00	52.00	52.00	63.00
Cell	type	Talc	Talc	NaCl	$BaCO_3$	Talc
	h.	31.70	31.70	31.70	31.70	43.00
	o.d.	12.70	12.70	12.70	12.70	18.80
	i.d.	11.20	10.00	10.00	8.00	13.00
Glass	type	Borosilicate	Borosilicate	Borosilicate	/	Borosilicate
	h.	31.70	31.70	30.50	/	43.00
	o.d.	11.20	10.00	10.00	/	13.00
	i.d.	8.00	8.00	8.00	/	10.00
Furnace	h.	30.50	30.50	30.50	31.80	41.70
	o.d.	8.00	8.00	8.00	8.00	10.00
	i.d.	6.00	6.00	6.00	6.00	8.00
Furnace lid	h.	1.20	1.20	1.20	/	1.30
	d.	8.00	8.00	8.00	/	10.00
Graphite lid	h.	1.65	1.65	1.40	1.65	1.50
	d.	12.70	12.70	12.70	12.70	18.90
Base plug	h.	12.75	13.75	13.40	12.75	12.60
	o.d.	10.70	10.70	10.70	10.70	17.00
Pyrophyllite sleeve	h.	12.75	13.75	13.40	12.75	12.60
	i.d.	10.70	10.70	10.70	10.70	17.00
	o.d.	12.70	12.70	12.70	12.70	18.90
Total	h.	46.10	47.10	46.50	46.10	57.10
Densiy of MgO spacers (kg/m^3)		2000	2000	2300	2800	2000

All dimensions in mm

h.: height

d. : diameter

o.d.: outer diameter

i.d.: inner diameter

Letters in parenthesis correspond to the labels on Figure 1.

501

Supplementary Material 2